Journal of the Korean Society of Groundwater Environment, Vol. 7, No. 2, pp. 59~65, June, 2000

A Study on the Liquefaction of Saturated Sand Layer under Oscillating Water Pressure
수압변동에 의한 포화 모래층의 액상화 연구

Howoong Shon(손호웅)* · Hyun-Chul Lim(임현철)** · Dae-Geun Lee(이대근)*

Abstract: The vertical distribution of pore water pressure in the highly saturated sand layer under the oscillating water pressure is studied theoretically and experimentally. By the experiments it is shown that the water pressure acting on the sand surface propagates into the sand layer with the damping in amplitude and the lag in phase, and that the liquefaction, the state that the effective stress becomes zero, occurs under certain conditions. These experimental results are explained fairly well by the same theoretical treatment as for the ground water problems in the elastic aquifer. The main characteristics of liquefaction clarified by the analysis are as follows: 1) The depth of the liquified layer increases with the increase of the amplitude and the frequency of the oscillating water pressure. 2) The increase of the volume of the water and the air in the layer increases the liquified depth. Especially the very small amount of the air affects the liquefaction significantly. 3) The liquified depth decrease rapidly with the increase of the compressibility coefficient of the sand. 4) In the range beyond a certain value of the permeability coefficient the liquified depth decrease with the increase of the coefficient.

요 약: 변동수압에 의한 포화 사질층의 연직 간극수압 분포를 이론 및 실험적으로 연구하였다. 실험에 의해 모래표면에 작용하는 수압은 모래층으로 전달되며 진폭이 감쇠하고 상이 지연되며, 유효응력이 0이 되는 액상화 현상이 특별조건에서 발생한다. 이러한 실험결과는 탄성 대수층에 대한 지하수문제와 같은 이론으로 잘 설명된다. 해석에 의한 액상화의 주요 특징은 다음과 같다: 1) 액상화 심도는 진폭 및 변동수압의 주파수 증가에 따라 증가한다. 2) 수량(水量)의 증가와 모래층 내의 공기가 많아짐에 따라 액상화 심도가 증가한다. 특히, 공기의 적은 양도 액상화에 크게 영향을 미친다. 3) 압축율이 증가함에 따라 액상화 심도는 감소한다. 4) 투수 계수값이 어느 특정값 이상이 되면 투수계수 값이 증가함에 따라 액상화 심도는 감소한다.

INTRODUCTION

Under the oscillating water pressure normal to the surface of the saturated sand layer, the pore water pressure in the layer changes with time and according to this circumstances the excess pore pressure occurs. The increase of the excess pore pressure brings to the decrease of the effective stress. Then, under certain conditions the effective stress becomes to be equal to zero, that is, the state of liquefaction occurs (Shon, 2000a). The liquified sand is removed easily by the flow tangential to the surface, and the sand layer will be scoured successively. Therefore, the clarification of the dynamical mechanism of such liquefaction is very important to design of hydraulic structures surrounded by the sand layer.

In this paper as a basic study for the explanation of the local scouring mechanism around the hydraulic structures and for the establishment of the prevention works against the scouring, the influence of the oscillating water pressure on the sand layer is investigated theoretically and experimentally.

* 배재대학교 토목환경공학과(Department of Civil and Geotechnical Engineering, Taejon 302-735, Korea)
** 한국자원연구소(Korea Institute of Geology, Mining and Materials, 30 Kajung-Dong, Yusung-Ku, Taejon 305-350, Korea)

Derivation of Fundamental Equation for Pore Water Pressure

To treat theoretically the vertically one-dimensional sand layer is considered as shown in Figure 1. The sand layer is highly saturated with water and is placed on the impermeable bed. The depth of the sand layer is D. The oscillating water pressure $\rho g h_s$ acts on the surface of the layer.

The behavior of water and sand in the sand layer is analyzed by the same method as for the ground-water problems in the elastic aquifer (Inoue, 1975; Kundu, 1990; Rouse, 1950; Shon, 1995). That is, it is assumed that sand and water are compressible, and then that the density of water, the porosity of the sand and the thickness of the layer are variable. But lateral strain of the sand is assumed to be negligible. The void in the sand layer is occupied by water

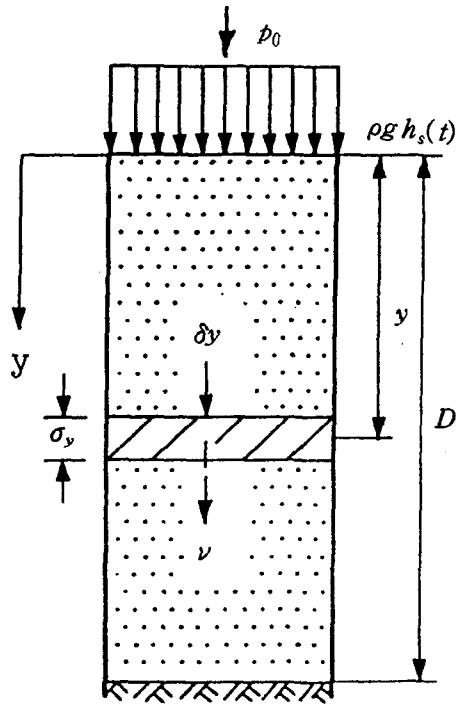

Figure 1. Sand layer under oscillating water (pressure).

and air. Then, the porosity λ is composed of the part for the water λ_W and the part for the air λ_a. The flow of water is considered through the faces of an elemental volume as shown in Figure 1. By the law of conservation of mass, the net inward flux must be equal to the rate at which water is accumulating within that volume. That is,

$$\frac{\partial}{\partial t}(\rho\lambda_W\delta y\delta A) = -\frac{\partial}{\partial y}(\rho v\delta A)\delta y \tag{1}$$

where ρ: density of water, v: velocity of flow, δA: horizontal cross-sectional area.

The left hand side of the above equation is transformed as follows:

$$\frac{\partial}{\partial t}(\rho\lambda_W\delta y\delta A) = \left(\lambda_W\frac{\partial\rho}{\partial t}\delta y + \rho\frac{\partial\lambda_W}{\partial t}\delta y + \rho\lambda_w\frac{\partial\delta y}{\partial t}\right)\delta A \tag{2}$$

The vertical dimension δy varies with the vertical component of compressive stress σ_y in accordance with,

$$d(\delta y) = -\alpha\delta y d\delta y \tag{3}$$

That is,

$$\frac{\partial(\delta y)}{\partial y} = -\alpha\delta y\frac{\partial\rho_y}{\partial t} \tag{4}$$

where α is the vertical compressibility of sand.

Since the compressibility of the individual sand grains is small compared to the compressibility of water and the change in the porosity, it can be considered that the volume of solid material remains constant (Shon, 2000a). That is

$$[1-(\lambda_W+\lambda_a)]\delta y\delta A = constant.$$

Differentiating the above equation by time variable t, the following equation is obtained.

$$\frac{\partial(\lambda_W+\lambda_a)}{\partial t} = -\alpha[1-(\lambda_W-\lambda_a)]\frac{\partial\sigma_y}{\partial t} \tag{5}$$

If the inertia force of the sand is negligibly small, the vertical component of compressive stress and the pore water pressure can be equated to the downward acting force on the plane of contact of the sand. That is,

$$\sigma_y + \rho gh = \gamma_g y + \rho gh_s \tag{6}$$

The pore water pressure ρgh and the weight of the sand column above the plane of contact $\lambda_s y$ are represented as follows:

$$\rho gh = \rho g(h_s + y + h') \tag{7}$$

$$\gamma_s y = \rho_s gy(1-l) + \rho gy\lambda_W \tag{8}$$

where h': excess pore water pressure, $\rho_s g$: weight of unit volume of the individual sand grain, g: acceleration due to gravity.

Substituting Eqs. (7), (8) into Eq. (6), and considering $\lambda_W \fallingdotseq \lambda$,

$$\rho_y + \rho gh' = (\rho_s-\rho)gy(1-\lambda) = constant \tag{9}$$

Accordingly,

$$\rho g\frac{\partial h'}{\partial t} = -\frac{\partial\sigma_y}{\partial t} \tag{10}$$

Then the following equation is obtained from Eqs. (4) and (10)

$$\frac{\partial\delta y}{\partial t} = \rho g\alpha\delta y\frac{\partial h'}{\partial t} \tag{11}$$

From Eqs. (5) and (10)

$$\frac{\partial(\lambda_W+\lambda_a)}{\partial t} = \rho g\alpha[1-(\lambda_W+\lambda_a)]\frac{\partial h'}{\partial t} \tag{12}$$

It is assumed that the volume of air in the layer changes in accordance with Boyle's law. That is,

$$\lambda_a\delta y\delta A(\rho gh+p_0) \approx \overline{\lambda_a}\delta y\delta A(\rho gh+p_0) = constant, \tag{13}$$

where p_0: atmospheric pressure, $\overline{\lambda_a}$: porosity occupied by the air under the standard pressure ($\overline{\rho gh}+p_0$).

Differentiating Eq. (13) by t, and using Eq. (10), the follow

equation is obtained.

$$\frac{\partial \lambda_a}{\partial t} = -\frac{\lambda_a}{\left(h+\frac{p_0}{\rho g}\right)}\frac{\partial h}{\partial t} - \rho g \alpha \lambda_a \frac{\partial h'}{\partial t} \tag{14}$$

From Eqs. (12), (14),

$$\frac{\partial \lambda_w}{\partial t} = \rho g \alpha (1-\lambda_w)\frac{\partial h'}{\partial t} + \frac{\lambda_a}{h+\frac{p_0}{\rho g}}\frac{\partial h}{\partial t} \tag{15}$$

The density of water changes in accordance with the following equation,

$$\frac{d\rho}{\rho} = \beta\, dp, p = \rho g h + p_0 \tag{16}$$

where β: compressibility of water, p: absolute pressure. Accordingly,

$$\frac{\partial \rho}{\partial t} = \beta \rho^2 g \frac{\partial h}{\partial t} \tag{17}$$

Substituting Eqs. (11), (15), (17) into Eq. (2),

$$\frac{\partial}{\partial t}(\rho \lambda_W \delta y \delta A) = \rho^2 g\left[\left(\beta \lambda_W + \frac{\lambda_a}{\rho g h + p_0}\right)\frac{\partial h}{\partial t} + \alpha \frac{\partial h'}{\partial t}\right]\delta y \delta A \tag{18}$$

It is assumed that the velocity of water in the layer follows Darcy's law (Kundu, 1990; Shon, 2000a, 2000b),

$$v = -k\frac{\partial h'}{\partial y} \tag{19}$$

where k is permeability coefficient.

Substituting Eqs. (18), (19) into Eq. (1) , finally the fundamental equation for the water pressure in the layer is obtained as follows:

$$\left(\beta \lambda_W + \frac{\lambda_a}{\rho g h} + p_0\right)\frac{\partial h'}{\partial t} + \left(\beta \lambda_W + \frac{\lambda_a}{\rho g h + p_0}\right)\frac{\partial h_s}{\partial t} = \frac{k}{\rho g}\frac{\partial^2 h'}{\partial y^2} \tag{20}$$

By solving the above equation under the following boundary conditions, the pore water pressure and the effective stress in the sand layer are obtained.

$$h' = 0 \quad at \quad y = 0 \tag{21}$$

$$\frac{\partial h'}{\partial y} = 0 \quad at \quad y = D$$

The liquefaction occurs under the following condition,

$$\frac{\sigma_v}{(\rho_s - \rho) g y (1-\lambda)} = 0 \tag{22}$$

For the case that the water pressure acting on the surface changes sinusoidally, that is,

$$h_s = h_0 + a_0 \sin 2\pi f t \tag{23}$$

Eq. (20) becomes,

$$\left(\beta \lambda_W + \frac{\lambda_a}{\rho g h + p_0} + \alpha\right)\frac{\partial h'}{\partial t} + 2\pi f a_0 \left(\beta \lambda_W + \frac{\lambda_a}{\rho g h + p_0}\right)\cos 2\pi f t = \frac{k}{\rho g}\frac{\partial^2 h'}{\partial y^2} \tag{24}$$

where h_0: head of mean water pressure on the sand surface, a_0: amplitude of oscillating water pressure, f: frequency of oscillating water pressure.

Eqs. (20) and (24) are nonlinear differential equation. Since it is difficult to solve these equations analytically, they are solved numerically.

Experiments on Liquefaction

Experimental procedure

For the experiment the vertical cylinder as shown in Figure 2 was used. The inside diameter of the cylinder is 8.9 cm and its height is 1.5 m. It is filled with the highly saturated sand up to about 43% of its height. The water depth from the sand surface is about 80 cm. The periodically oscillated air pressure acts on the water surface. Its amplitude is 95 cm in

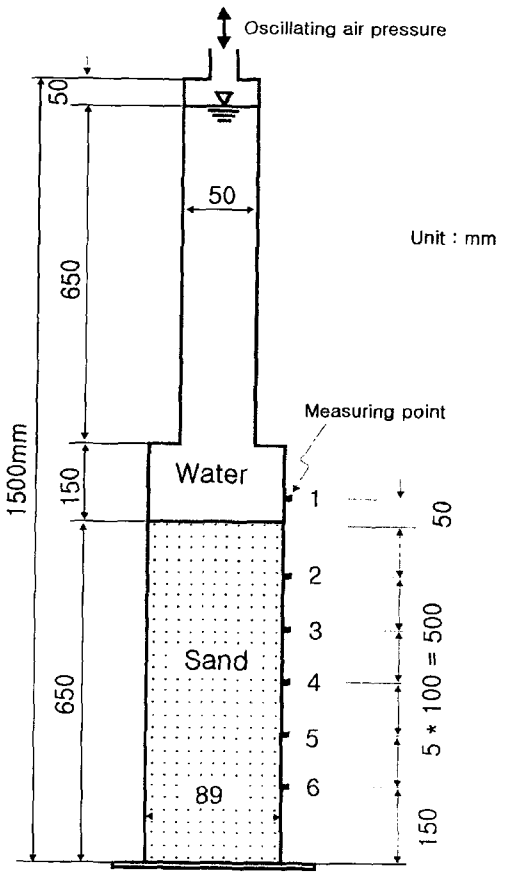

Figure 2. Experimental Model.

water head. The frequency changes from 1.37 Hz to 5.66 Hz. The nearly uniform sand which 50% of grain size is 0.25 mm was used. Two kinds of sand sample concerning to the volume of air in the layer was used. That is, the one is the sample which $\overline{\lambda_a}$ is about 0.5% at $\bar{h}$=0.3 m and the other is the sample which $\overline{\lambda_a}$ is very small comparing with the former sample. In the following description each sample is called the aerated and the deaerated sample respectively. The value of $\overline{\lambda_w}$ is about 40%. The coefficient of permeability is about 2×10^{-2} cm/s. The water pressures in the water and sand layer are measured by the semi-conductor pressure transducer attached to the side of the cylinder.

Experimental results

In Figures 3(a) and (b), the changes of the pore water pressure for the deaerated and aerated sands are shown. These figures show that water pressure on the sand surface propagates into the sand layer accompanied with the damping in amplitude and the lag in phase. The damping rate and lag in the aerated sand is larger than those in the deaerated sand. Figures 4(a) and (b) show the damping ratio of the amplitude for both samples. The symbol a in the figures represents the amplitude in the sand layer. These figures show that the amplitude decreases with increasing frequency. Figures 5(a) and (b) show the change of the effective stress, and that the

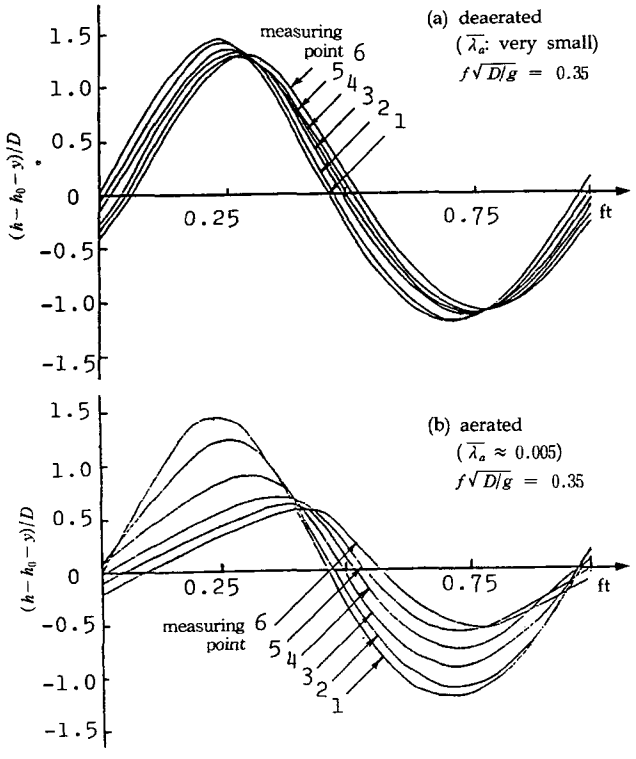

Figure 3. Observed pore water pressure.

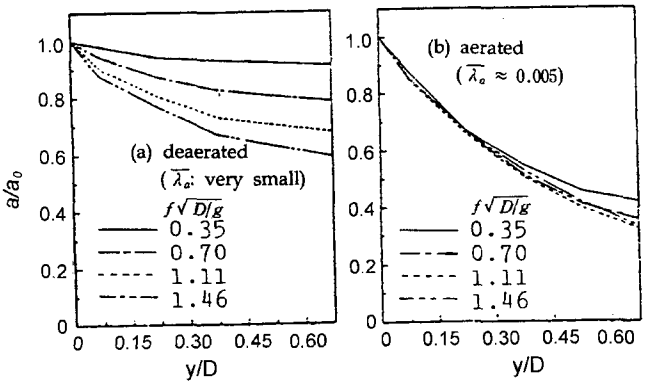

Figure 4. Observed damping ratio of amplitude.

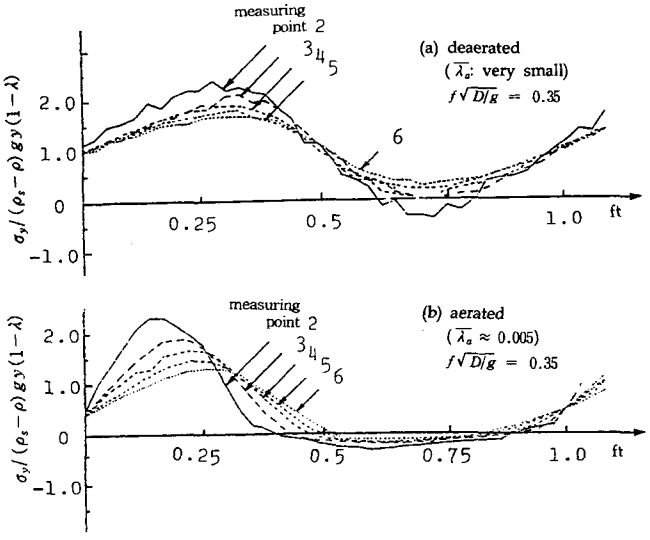

Figure 5. Observed effective Stress.

state of the liquefaction (σ_y=0) appears at the point 1 for the deaerated sample and at all measuring points for the aerated one. Figures 6, 7 and 8 show the calculated curves of the pore water pressure, the damping ratio and the effective stress corresponding to Figures 3, 4 and 5, respectively. In the calculation it is assumed that the compressibility of sand α is 1.8×10^{-6} cm^2/g. The calculated curves match fairly well with the experimental results. The differences between the experimental results and the calculated curves are considered to be mainly due to the approximation of the oscillating water pressure and the compressibility in the calculation.

Characteristics of Liquefaction

Factors affecting liquefaction

The characteristics of the liquefaction depend on the properties of water, sand layer, oscillating water pressure and field conditions. For convenience adopting the sinusoidal excitation like Eq. (23) as the oscillating water pressure, the characteristic parameters influencing on the phenomenon are

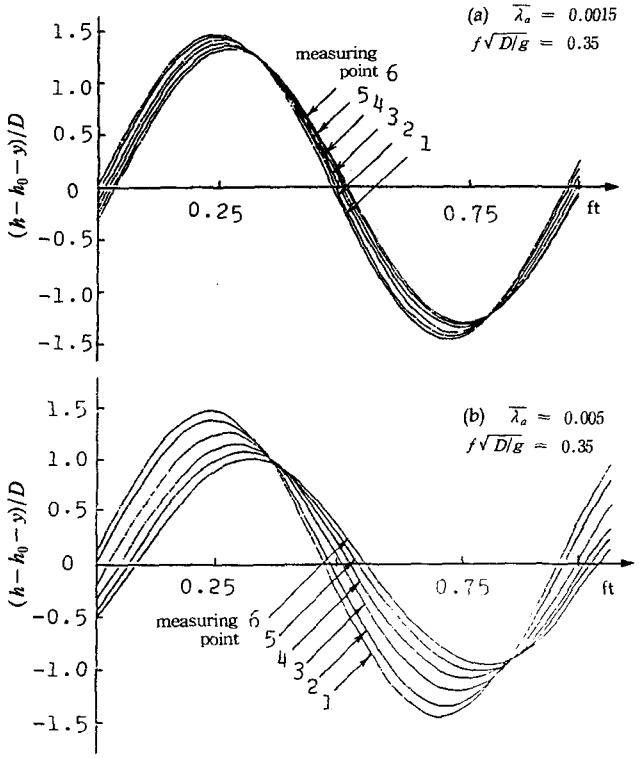

Figure 6. Calculated pore water pressure.

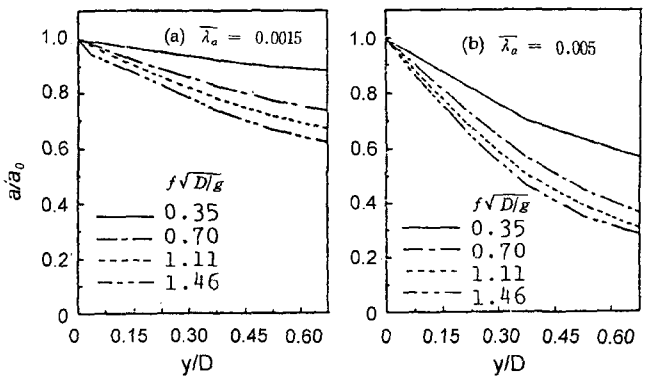

Figure 7. Calculated damping ratio of amplitude.

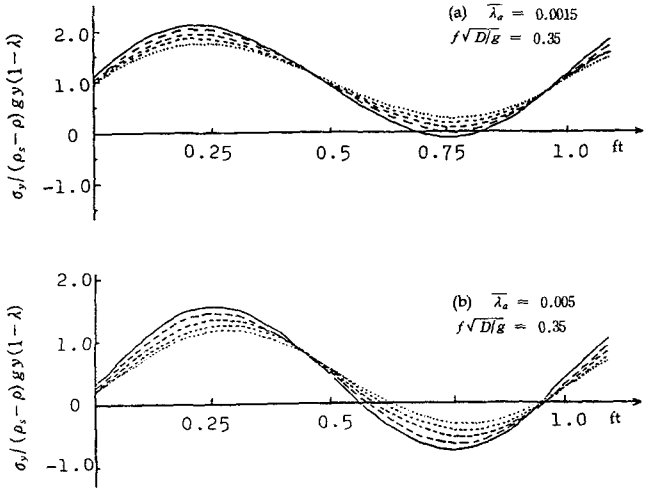

Figure 8. Calculated effective Stress.

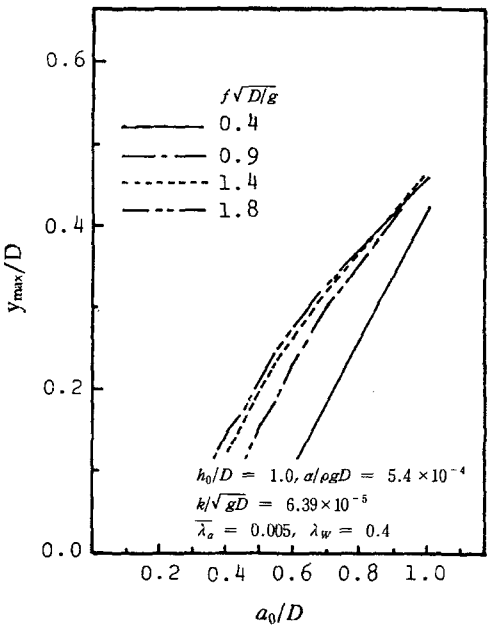

Figure 9. a_0/D vs. y_{max}/D.

as follows:

1) water: ρ, β; 2) sand layer: ρ_s, α, λ_W, $\bar{\lambda}_a$, k, D, $\bar{h}$; 3) water pressure: a_0, f, h_0; 4) field condition: g, p_0.

Accordingly the quantitative property A of the liquefaction is given by the following functional relation.

$$A = F(a_0, f, h_0, \rho_s, \alpha, \lambda_W, \bar{\lambda}_a, k, D, \rho, \beta, g, h_y, t) \tag{25}$$

By the dimensional analysis using ρ, g and D as the fundamental quantities of dimensions the above equation is transformed to,

$$\pi_A = \Phi\left(\frac{a_0}{D}, f\sqrt{\frac{D}{g}}, \frac{h_0}{D}, \frac{\rho_s}{\rho}, \alpha(\rho gD), \lambda_W, \bar{\lambda}_a, \frac{k}{\sqrt{gD}}, \beta(\rho gD),\right.$$

$$\left.\frac{p_0}{\rho gD}, \frac{\bar{h}}{D}, \frac{y}{D}, t\sqrt{\frac{g}{D}}\right) \tag{26}$$

Maximum depth of liquified layer

Here the maximum depth of the liquified sand layer y_{max} is dealt as one of the properties of liquefaction, and analyzed theoretically under the following conditions,

$$\rho_s/\rho = 2.65, \bar{h}/D = 0.3, p_0/\rho gD = 10.3$$

$$\beta(\rho gD) = 0.41 \times 10^{-5}$$

In Figures 9 to 14, the changes of the maximum depth y_{max} with a_0/D, λ_a, λ_W, $k/\sqrt{gD}$, $\alpha(\rho gD)$ and h_0/D are shown with the parameter $f\sqrt{D/g}$.

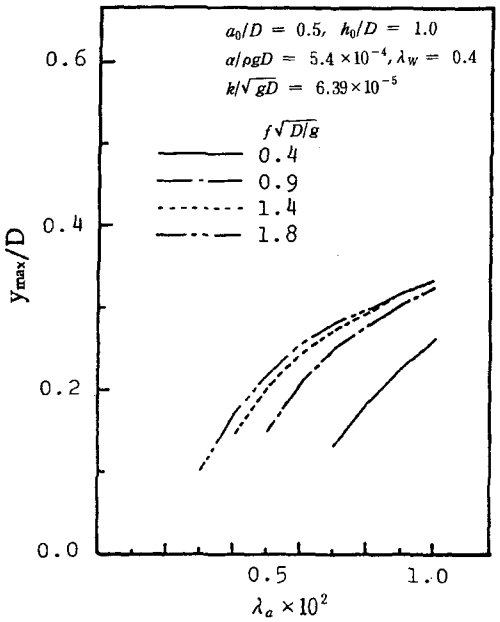

Figure 10. λ_0/D vs. y_{max}/D.

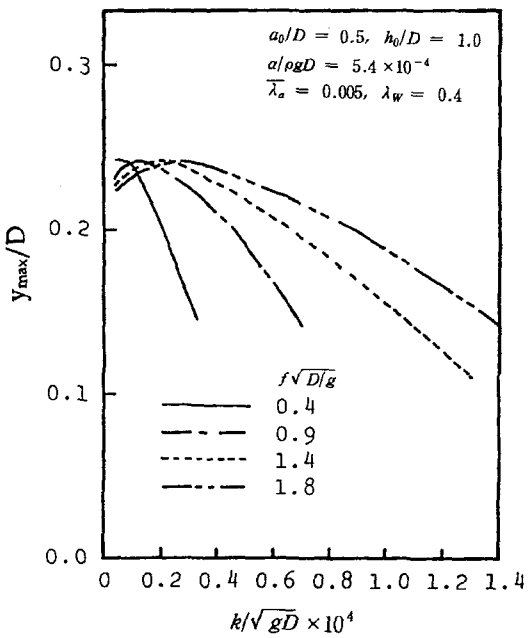

Figure 12. k/gD vs. y_{max}/D.

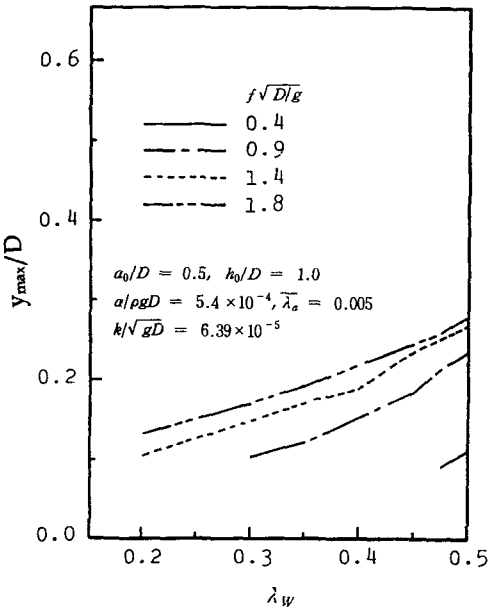

Figure 11. λ_0/D vs. y_{max}/D.

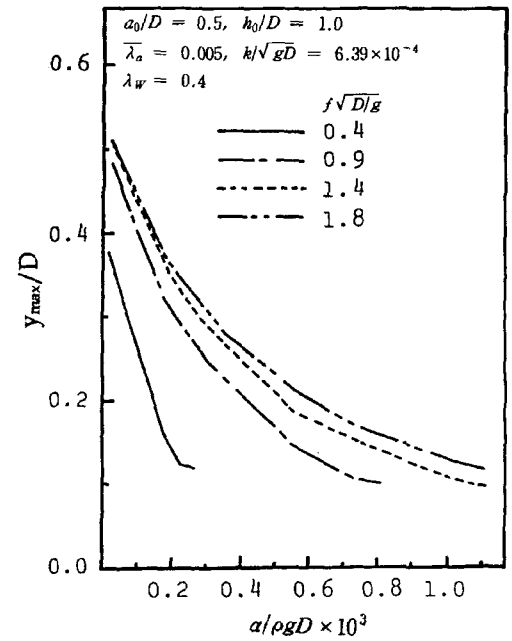

Figure 13. $\alpha/\rho gD$ vs. y_{max}/D.

Figures 9, 10 and 11 show y_{max} increases with the increase of $a_0/D, \lambda_a, \lambda_W$ and frequency. Especially a very small amount of air in the sand affects the liquefaction considerably.

Figure 12 shows that y_{max} decreases with the increase of the coefficient of permeability beyond certain value of the coefficient. Figure 13 shows that y_{max} decreases rapidly with the increase of the compressibility of the sand. Figure 14 shows that the increase of the mean water pressure decreases the liquified depth, although its degree is very small.

Conclusion

From the experiments and the theoretical analysis, following conclusions are achieved: 1)Experiments show that the oscillating water pressure acting on the surface of the highly saturated sand layer propagates into the layer with the damping in amplitude and the lag in phase, and that under certain conditions the liquefaction appears. It is obvious that

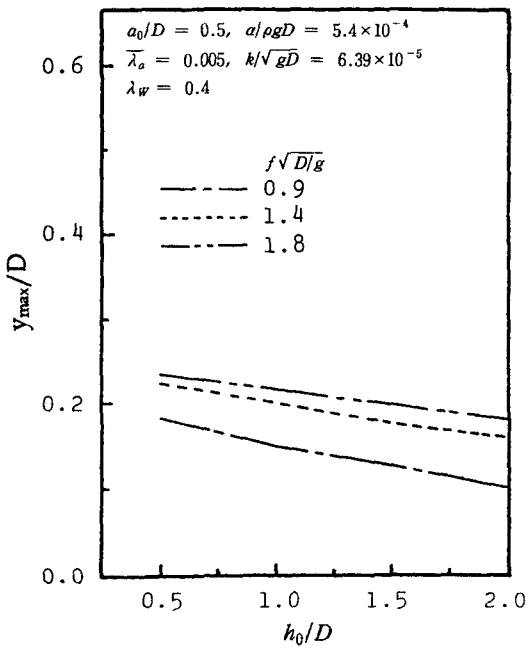

Figure 14. h_0/D vs. y_{max}/D.

the damping ratio and the phase lag depend mainly on the volume of the air involved in the layer. These experimental results are matched fairly well with the theoretical analysis. 2)By the theoretical analysis several properties on the liquefaction are obtained as follows: The maximum depth of liquified layer increases with the increase of the amplitude and the frequency of the oscillation water pressure and the volume occupied by the air and the water in the sand layer. Especially a small amount of the air affects on the liquefaction significantly. The increase of the coefficient of permeability beyond certain value decreases the depth of liquefaction. With the increase of the mean water pressure and the compressibility of the sand, the liquified depth decrease.

Acknowledgement

The authors extend their gratitudes to Prof. Shiro Maeno in the Dept. of Civil and Environmental Engineering at Okayama University, Japan, and Prof. Tokuo Yamamoto in the Division of Applied Marine Physics at the University of Miami, USA for their review and supports to experiment by allowing to use the state-of-art laboratory. This study is funded from KOSEF 98-0703-02-01-3 and Korea Research Fund DP0434.

References

Inoue, R., 1975, Propagation of pore water pressure in sand layer of high degree of saturation, Proc. JSCE, No. 236.

Kundu, P. K., 1990, Fluid Mechanics. Academic Press.

Rouse, H., 1950, Engineering Hydraulics. John Willey & Sons.

Shon, H., 1995, Reconstruction of the Wave Speed and Density from Reflection Coefficients by Downward Continuation Algorithm. Econ. Eviron. Geol., 28(6), p. 553-558

Shon, H. and Jeong, G. C., 2000a, Results Analyses and Application of Ground Investigation and Soil Test, Pub. of Engineers.

Shon, H., Woo, N. C., Kim, J. S., Lee, D. H., Sung, I. H., Jeong, G. C., Ham, S. Y. and Lee, H. S., 2000b, Applied Groundwater.